Available online at www.sciencedirect.com

ScienceDirect

Dyes and Pigments 74 (2007) 262–268

DYES and PIGMENTS

www.elsevier.com/locate/dyepig

# Dichromophoric hemicyanine dyes. Synthesis and spectroscopic investigation

Beata Jędrzejewska*, Janina Kabatc, Jerzy Pączkowski

*Faculty of Chemical Technology and Engineering, University of Technology and Agriculture, Seminaryjna 3, 85-326 Bydgoszcz, Poland*

Received 4 November 2005; received in revised form 2 February 2006; accepted 6 February 2006

## Abstract

The new dyes, xylene-1,4-bis[4-(*p*-aminostyryl)-pyridinium bromide] derivatives, have been synthesized and their spectroscopic properties were investigated. These dyes are stilbene-type pyridinium salts that possess in their structure different electron donor groups. We compile here the electronic absorption and the emission spectra properties as well the fluorescence quantum yields measured in organic solvents of varying polarity. The UV–vis and steady-state fluorescence spectroscopic investigations show the solvent-sensitive absorption and emission, which result from the intramolecular charge transfer (ICT) nature of the chromophores present in the dendritic structure.

*Keywords:* Dichromophoric hemicyanine dye; Synthesis; Absorption and emission spectra; The Stokes shift

## 1. Introduction

Aminostyrylpyridinium salts (hemicyanine dyes) which possess the electron pushing (donor) group on one end and the electron withdrawing (acceptor) group on the other end have found a successful application in science and technology. These chromophores are common fluorescence probes used in biochemistry and biophysical areas [1]. They are also very commonly applied to lasers [2], electronics [3], and nonlinear optics [4].

In recent years, there have been quite a few reports on dichromophoric dyes [5,6] which possess very attractive photophysical characteristics for the above mentioned applications. Dichromophoric cyanine dyes have two positive charges in their structure. Usually, the dimerization of the chromophores causes various changes in steady-state absorption and fluorescence spectra. These changes, especially the maximum shifts, can be easily interpreted by the formation of intramolecular aggregates or by the interchromophore charge delocalization [7]. However, no such kind of interaction is observed for the hemicyanine dimmers with xylene group as the linker studied in our research.

In this paper, we describe the design and synthesis of a series of dichromophoric stilbene-type derivatives in which the terminal substituted amino groups are used as electron donors. The effect of the dyes' structure on their spectroscopic properties is discussed as well.

## 2. Experimental

### 2.1. Measurements

All starting reagents and solvents (reagent grade) were purchased from Aldrich Chemical Co. and used without further purification. Aldehydes, as substrates for synthesis of dichromophoric dyes were synthesized according to the procedure given by Gawinecki et al. [8].

The $^1$H NMR spectra were recorded with the use of a Varian spectrometer Gemini 200 operating at 200 MHz.

---

* Corresponding author. Tel.: +48 52 374 9045; fax: +48 52 374 9009.
*E-mail address:* beata@atr.bydgoszcz.pl (B. Jędrzejewska).

0143-7208/$ - see front matter © 2006 Elsevier Ltd. All rights reserved.
doi:10.1016/j.dyepig.2006.02.003

Dimethylsulfoxide (DMSO) was used as the solvent and tetramethylsilane (TMS) as the internal standard.

Melting points (uncorrected) were determined on the Boëthius apparatus.

For the measurements of the electronic absorption and emission spectra, as well the fluorescence quantum yield ($\Phi$), the $1.0 \times 10^{-5}$ M dye solutions in both acetonitrile (MeCN) and dichloromethane (DCMe) were prepared. At such a concentration, no aggregation or self-absorption effects of the dyes were observed [9]. Absorption spectra were recorded at room temperature using a Shimadzu UV–vis Multispec-1501 spectrophotometer, and fluorescence spectra were obtained with a Hitachi F-4500 spectrofluorimeter. The fluorescence measurements were performed at an ambient temperature.

The fluorescence quantum yields for the dyes in MeCN and DCMe were determined as follows. The fluorescence spectrum of a dilute (<25 μM) dye solution was recorded by excitation at the absorption band maximum of the standard. A dilute Rhodamine B in ethanol ($\Phi = 0.55$ [10]) was used as reference. The fluorescence spectrum of Rhodamine B was obtained by excitation at its absorption maximum at 530 nm. The quantum yield of the tested dye ($\Phi_{\mathrm{dye}}$) was calculated using the equation:

$$\Phi_{\mathrm{dye}} = \Phi_{\mathrm{ref}} \frac{I_{\mathrm{dye}} A_{\mathrm{ref}}}{I_{\mathrm{ref}} A_{\mathrm{dye}}} \qquad (1)$$

where $\Phi_{\mathrm{ref}}$ is the fluorescence quantum yield of reference (Rhodamine B) sample in ethanol, $A_{\mathrm{dye}}$ and $A_{\mathrm{ref}}$ are the absorbances of the dye and reference samples at the excitation wavelengths (530 nm), $I_{\mathrm{dye}}$ and $I_{\mathrm{ref}}$ are the areas' arbitrary units of the corrected fluorescence spectra (plotted in frequency scale) for the dyes and reference samples, respectively.

## 2.2. Synthetic procedure

### 2.2.1. Xylene-1,4-bis[4-methylpyridinium bromide]

A mixture of 1,4-di-(bromomethyl)benzene (0.01 mol, 2.64 g) and γ-picoline (0.02 mol, 1.86 g, 1.95 mL) in anhydrous ethanol (100 mL) was refluxed for 4 h. After cooling to room temperature the precipitated white solid was filtered, washed with $Et_2O$ and dried (yield 60%) [11].

### 2.2.2. General procedure for synthesis of xylene-1,4-bis[4-(*p*-aminostyryl)-pyridinium bromide] derivatives

Xylene-1,4-bis[4-(*p*-aminostyryl)-pyridinium bromide] derivatives were obtained by refluxing (1–2 h) the proper *p*-aminobenzaldehyde (4 mmol) with xylene-1,4-bis[4-methylpyridinium bromide] (2 mmol, 0.9 g) in methanol (20 mL) in the presence of piperidine (few drops). The precipitate formed after cooling down the reaction mixture was filtered and crystallized from MeOH/isopropyl alcohol to yield (usually about 50%) the desired dye usually as a red solid [11]. The products were identified spectroscopically.

#### 2.2.2.1. Dye ***A1*** – *xylene-1,4-bis[4-(p-(N,N-dimethylamino)-styryl)-pyridinium bromide]*

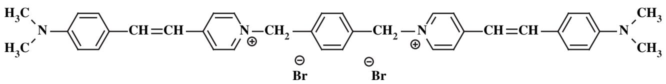

The dye was prepared by the procedure described above using xylene-1,4-bis[4-methylpyridinium bromide] (2 mmol, 0.9 g) and *p*-(*N*,*N*-dimethylamino)benzaldehyde (4 mmol, 0.6 g). The red solid was crystallized from methanol/isopropyl alcohol; 0.85 g, yield 62%.

#### 2.2.2.2. Dye ***A2*** – *xylene-1,4-bis[4-(p-(N,N-diethylamino)-styryl)-pyridinium bromide]*

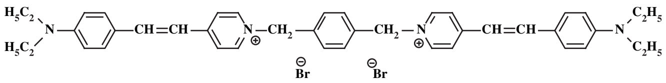

The dye was prepared by applying the procedure described above using xylene-1,4-bis[4-methylpyridinium bromide] (2 mmol, 0.9 g) and *p*-(*N*,*N*-diethylamino)benzaldehyde (4 mmol, 0.7 g). The red solid was crystallized from methanol/isopropyl alcohol; 0.65 g, yield 47%.

#### 2.2.2.3. Dye ***A3*** – *xylene-1,4-bis[4-(2-methyl-p-(N,N-dimethylamino)styryl)-pyridinium bromide]*

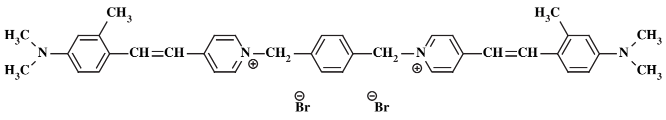

The dye was prepared according to the procedure described above using xylene-1,4-bis[4-methylpyridinium bromide] (2 mmol, 0.9 g) and 3-methyl-*p*-(*N*,*N*-dimethylamino)benzaldehyde (4 mmol, 0.65 g). The yielded red solid was crystallized from methanol/isopropyl alcohol; 0.83 g, yield 61%.

#### 2.2.2.4. Dye ***A5*** – *xylene-1,4-bis[4-(p-pyrrolidinostyryl)-pyridinium bromide]*

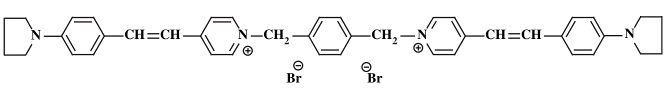

The dye was prepared by applying the procedure described above using xylene-1,4-bis[4-methylpyridinium bromide]

(2 mmol, 0.9 g) and 4-pyrrolidinobenzaldehyde (4 mmol, 0.7 g). The resulting red solid was crystallized from methanol/isopropyl alcohol; 0.95 g, yield 69%.

### 2.2.2.5. Dye **A6** – *xylene-1,4-bis[4-(p-piperidinostyryl)-pyridinium bromide]*

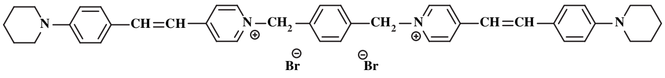

For the preparation of the dye, the general procedure described above was applied. As substrates xylene-1,4-bis[4-methylpyridinium bromide] (2 mmol, 0.9 g) and 4-piperidinobenzaldehyde (4 mmol, 0.76 g) were used. The obtained red solid was crystallized from methanol/isopropyl alcohol; 1.07 g, yield 72%.

### 2.2.2.6. Dye **A7** – *xylene-1,4-bis[4-(2-(N-metylo-5,6-dihydroindolino)etyleno)-pyridinium bromide]*

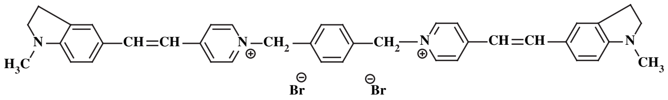

The desired dye was prepared based on the general procedure using xylene-1,4-bis[4-methylpyridinium bromide] (2 mmol, 0.9 g) and 1-methylindolino-4-aldehyde (4 mmol, 0.64 g) as substrates. The obtained red solid was crystallized from methanol/isopropyl alcohol; 0.85 g, yield 61%.

### 2.2.2.7. Dye **A8** – *xylene-1,4-bis[4-(2-(N-metylo-4,5,6-trihydrochinolino)etyleno)-pyridinium bromide]*

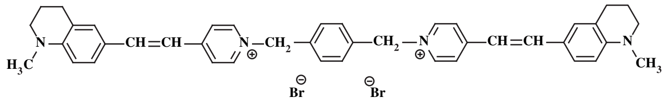

For the synthesis of the dye xylene-1,4-bis[4-methylpyridinium bromide] (2 mmol, 0.9 g) and 1-methyl-1,2,3,4-tetrahydrochinolino-4-aldehyde (4 mmol, 0.7 g) were used as substrates. The red solid was crystallized from methanol/isopropyl alcohol; 0.78 g, yield 57%.

### 2.2.2.8. Dye **A9** – *xylene-1,4-bis[4-(2-(julolidyno)etyleno)-pyridinium bromide]*

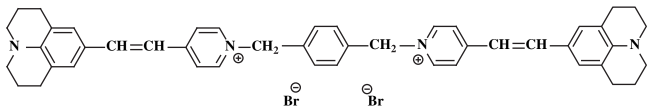

The dye was prepared by applying the methodology given in the general procedure using xylene-1,4-bis[4-methylpyridinium bromide] (2 mmol, 0.9 g) and julolidyno-4-aldehyde (4 mmol, 0.8 g) as substrates. The yielded red solid was crystallized from methanol/isopropyl alcohol; 0.94 g, yield 61%.

## 3. Results and discussions

### 3.1. Molecular design and synthetic procedures

Eight dichromophoric, possessing two identical chromophores, dyes have been synthesized by the reaction of xylene-1,4-bis[4-methylpyridinium bromide] by Knoevenagel condensation with proper *p*-aminobenzaldehyde [11]. The reaction was carried out in methanol using piperidine as catalyst. The general route for the synthesis of the xylene-1,4-bis[4-(*p*-aminostyryl)-pyridinium bromide] derivatives is presented in Scheme 1.

Details of the synthetic procedures and structures of tested dyes (see Scheme 1) are described in Section 2. The dyes were purified by crystallization from appropriate solvent mixtures. The structure and purity of the prepared compounds were confirmed by $^1$H NMR spectroscopy and thin layer chromatography. The data of the structural analysis for all dyes are given in Table 1. It is noteworthy that the $^1$H NMR spectra (Table 1) display two characteristic doublets localized at chemical shifts about 7 and 8 ppm. They are attributed to both vinyl hydrogen atoms. Based on the large coupling constant for the olefinic protons ($J_{cd}$ = 15–16 Hz) it is concluded that these dyes exist as all-*trans* conformation in the ground state.

### 3.2. Spectroscopic studies

Absorption spectra always reflect molecular interactions, especially those between two or more chromophores. If there are molecular aggregates in the system, then the absorption spectroscopic method is almost the most powerful technique for identifying them [7]. We are not observing the absorption shift when the concentration of the solution changes. That is to say, in the solution, the aggregation can be ignored. The electronic absorption spectra of tested dyes in acetonitrile are shown in Fig. 1. Evidently, there are no dramatic differences in the electronic absorption spectra of the dyes under the study. UV–vis spectroscopic measurements of tested dimmers (Fig. 1) show broad absorption bands in the range of 480–580 nm corresponding to the $S_0 \rightarrow$ CT transition attributed to an intramolecular charge transfer (ICT) involving the electron lone pair of the amino nitrogen and the cationic pyridinium nitrogen moiety [12,13]. The shortest wavelength bands are attributed to the $\pi \rightarrow \pi^*$ transitions.

The molar absorption coefficient of tested dyes is about twice as high as for their monomeric equivalents.

The inspection of the absorption spectra presented in Figs. 1 and 2 shows that the position of the CT absorption band depends on the molecular structure of the dye. In both solvents tested the maximum absorption position (Table 2) differs in some cases up to 50 nm and this indicates that the electronic transition of the hemicyanine dimmers is

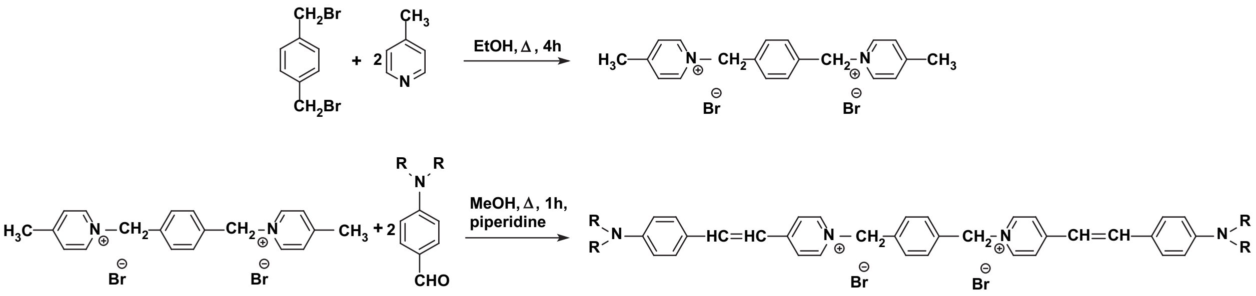

Scheme 1. A general route for the synthesis of the xylene-1,4-bis[4-(*p*-aminostyryl)-pyridinium bromide] derivatives.

caused by the structure of the electron donor moiety. A good illustration of this influence is shown by the dyes **A9** and **A1**. Dye **A9** absorption bands' maxima are located at 565 nm in DCMe and at 538 nm in MeCN, whereas **A1** absorption bands' maxima are present at 512 and 487 nm, respectively. This bathochromic effect could be attributed to the rigid and planar structure of the amino group with respect to benzene ring. This causes an increase in the delocalization of the lone pair electron at the amino nitrogen to the π-orbital of the dye chromophore cation [14]. In general, the better the electron donor is substituted, the more bathochromically the CT absorption band is shifted.

It is also observed (Fig. 2) that the monochromophoric dye (**M1**) (4-(*p*-(*N*,*N*-dimethylamino)styryl)-pyridinium perchlorate) shows in DMF $\lambda_{max}$ at 469 nm, while its dichromophoric equivalents (**A1**) show absorption maxima at 488 nm. The mechanism causing the red shift observed for dichromophoric dyes in comparison to its monomeric equivalents is not clear. It may be speculated that the second electron acceptor, being in proximity to one belonging to light absorbing chromophore, causes an additional increase of electron affinity of the electron-accepting moiety of light absorbing chromophore. The results supporting this hypothesis may come from the paper published by Huang et al. who described the properties of similar types of dichromophoric hemicyanine dyes [15]. These authors have documented that the red shift of the absorption maximum for the dichromophoric dyes in comparison to monochromophoric ones is decreasing as the number of methylene units separating the chromophores is increasing. The red shift (in DMF) for the dye with three methylene units is about 700 $\mathrm{cm^{-1}}$, for five units about 340 $\mathrm{cm^{-1}}$ and for 12 units only 90 $\mathrm{cm^{-1}}$. The specific influence of the neighboring electron-accepting group on light absorbing molecule may have crucial importance on possible two-photon absorption properties of the dyes described in this paper.

Because of their strong charge transfer character, the absorption spectra, it is shown in Fig. 3, are influenced by the medium polarity.

The negative solvatochromism of the tested compounds has been observed in the absorption (absorption peak position shifts to the blue as solvent polarity increases). This shift can be as high as 1000 $\mathrm{cm^{-1}}$ and indicates that the ground state may have greater dipole moments than the Franck–Condon excited state.

The dimmers under study are ionic dyes which exhibit a dipolar character in the ground state. The solvent molecules are oriented in a way required by the dipolar character of the host molecule. During the transition, which occurs within a very small time interval, only the electrons have the time to change position. The excited molecules, in which the electric dipole has been weakened and has been reoriented, are now within a solvent cage that is no longer adopted to the electronic requirements of the excited molecule, since the solvent cage is suitable for the electronic distribution in the ground state molecule. Thus, a polar solvent creates a stabilizing solvent cage around these ionic dyes in the ground state, but a destabilizing solvent cage for the excited state. The transition energy increases with increasing solvent polarity. An increase in solvent polarity results in hypsochromic shift of the charge transfer band, i.e. to shorter wavelengths.

The absorption and fluorescence maxima and the molar absorption coefficients for the eight different dyes under study in acetonitrile and dichloromethane are compiled in Table 2.

The dyes show broad structureless emission spectra with large Stokes shift. The emission data are given in Table 2. Fig. 4 depicts the emission spectra for the selected dyes in dichloromethane.

All dimmers show similar one-band fluorescence spectra. The illustrative fluorescence spectra, presented in Fig. 4, suggest that the structure of the molecule electron donor group affects the position and intensity of the emission band. The rigidity and planarization of the amino group leads to the red shift in the fluorescence (see Table 2).

Fluorescing molecules with rigid ring structures (like anthracene) retain the same structure in the ground and excited states in any organic solvents. Fluorescent molecules such as the studied ones have the possibility of multiple structure formation caused by the possibility of the molecule fragments' rotation about bonds linking molecule various moieties. Stokes shift is one of the quantitative parameters which is useful for understanding the origin of the variation of spectral shift in organic solvents and is an important characteristic of change of the dipole moment upon excitation and thus indicates the extent of charge transfer in the excited state [16].

It is apparent from the inspection of the spectra presented in Fig. 3 and data collected in Table 2 that there is a significant variation in the spectral peak position and Stokes shift caused by the change of the solvent polarity. The fluorescence

Table 1
Characteristics of the bichromophoric hemicyanine dyes tested

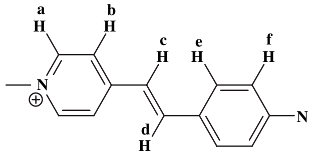

| Dye | Empirical formula | Molecular mass (g/mol) | M.p. (°C) | $^1$H NMR (DMSO) $\delta$ (ppm) |
|---|---|---|---|---|
| **A1** | $C_{38}H_{40}N_4Br_2$ | 712 | 281–290 | 2.581 (s, 3H, $-CH_3$), 3.014 (s, 9H, $-CH_3$), 5.657 (s, 2H, $N^+CH_2-$), 5.776 (s, 2H, $N^+CH_2-$), 7.117–7.198 (d, $J_{cd} = 16.2$ Hz, 2H, $-CH=$), 7.879–7.960 (d, $J_{cd} = 16.2$ Hz, 2H, $-CH=$), 6.750–6.795 (d, $J_{ef} = 9$ Hz, 4H, Ar), 7.562–7.603 (d, $J_{ef} = 8.2$ Hz, 8H, Ar), 7.971–8.003 (d, $J_{ab} = 6.4$ Hz, 2H, Pyr), 8.038–8.073 (d, $J_{ab} = 7$ Hz, 2H, Pyr), 8.839–8.873 (d, $J_{ab} = 6.8$ Hz, 2H, Pyr), 9.008–9.041 (d, $J_{ab} = 6.6$ Hz, 2H, Pyr) |
| **A2** | $C_{42}H_{48}N_4Br_2$ | 768 | 200–212 | 1.078–1.147 (t, 12H, $-CH_3$), 2.583 (s, 4H, $-CH_2-$), 3.184 (s, 4H, $-CH_2-$), 5.647 (s, 2H, $N^+CH_2-$), 5.775 (s, 2H, $N^+CH_2-$), 7.066–7.147 (d, $J_{cd}$=16.2 Hz, 2H, $-CH=$), 7.861–7.940 (d, $J_{cd} = 15.8$ Hz, 2H, $-CH=$), 6.715–6.759 (d, $J_{ef} = 8.8$ Hz, 4H, Ar), 7.532–7.575 (4H, Ar), 7.618–7.663 (d, $J_{ef} = 9$ Hz, 4H, Ar), 7.971–8.006 (d, $J_{ab} = 7$ Hz, 2H, Pyr), 8.017–8.052 (d, $J_{ab} = 7$ Hz, 2H, Pyr), 8.813–8.848 (d, $J_{ab} = 7$ Hz, 2H, Pyr), 9.009–9.042 (d, $J_{ab} = 6.6$ Hz, 2H, Pyr) |
| **A3** | $C_{40}H_{44}N_4Br_2$ | 740 | 201–210 | 2.440 (s, 3H, $-CH_3$), 2.584 (s, 3H, $-CH_3$), 2.710 (s, 3H, $-CH_3$), 2.999 (s, 9H, $-CH_3$), 5.661 (s, 2H, $N^+CH_2-$), 5.767 (s, 2H, $N^+CH_2-$), 7.084–7.164 (d, $J_{cd} = 16$ Hz, 2H, $-CH=$), 7.976–8.058 (d, $J_{cd} = 16.4$ Hz, 2H, $-CH=$), 6.578–6.660 (4H, Ar), 7.554–7.567 (4H, Ar and 2H Pyr), 7.687–7.732 (d, $J_{ef} = 9$ Hz, 2H, Ar), 8.099–8.134 (d, $J_{ab} = 7$ Hz, 2H, Pyr), 8.814–8.849 (d, $J_{ab} = 7$ Hz, 2H, Pyr), 8.996–9.028 (d, $J_{ab} = 6.4$ Hz, 2H, Pyr) |
| **A5** | $C_{42}H_{44}N_4Br_2$ | 764 | 247–251 | 1.969 (t, 8H, $-CH_2-$), 2.583 (s, 4H, $-CH_2-$), 3.175 (s, 4H, $-CH_2-$), 5.639 (s, 2H, $N^+CH_2-$), 5.767 (s, 2H, $N^+CH_2-$), 7.078–7.158 (d, $J_{cd} = 16$ Hz, 2H, $-CH=$), 7.869–7.948 (d, $J_{cd} = 15.8$ Hz, 2H, $-CH=$), 6.598–6.641 (d, $J_{ef} = 8.6$ Hz, 4H, Ar), 7.554–7.596 (8H, Ar), 8.008–8.044 (d, $J_{ab} = 7.2$ Hz, 2H, Pyr), 8.803–8.837 (d, $J_{ab} = 6.8$ Hz, 4H, Pyr), 8.995–9.029 (d, $J_{ab} = 6.8$ Hz, 2H, Pyr) |
| **A6** | $C_{44}H_{48}N_4Br_2$ | 792 | 222–230 | 1.043 (s, 4H, $-CH_2-$), 1.581 (t, 8H, $-CH_2-$), 2.583 (s, 4H, $-CH_2-$), 2.984 (s, 4H, $-CH_2-$), 5.673 (s, 2H, $N^+CH_2-$), 5.777 (s, 2H, $N^+CH_2-$), 7.154–7.235 (d, $J_{cd} = 16.2$ Hz, 2H, $-CH=$), 7.870–7.951 (d, $J_{cd} = 16.2$ Hz, 2H, $-CH=$), 6.960–7.004 (d, $J_{ef} = 8.8$ Hz, 4H, Ar), 7.566–7.594 (8H, Ar), 8.064–8.099 (d, $J_{ab} = 7$ Hz, 2H, Pyr), 8.868–8.901 (d, $J_{ab} = 6.6$ Hz, 2H, Pyr), 9.009–9.042 (d, $J_{ab} = 6.6$ Hz, 4H, Pyr) |
| **A7** | $C_{40}H_{40}N_4Br_2$ | 736 | 198–204 | 2.583 (t, 4H, $-CH_2-$), 2.823 (s, 3H, $-CH_3$), 2.926–3.008 (t, 3H, $-CH_3$), 3.471–3.512 (t, 4H, $-CH_2-$), 5.654 (s, 2H, $N^+CH_2-$), 5.784 (s, 2H, $N^+CH_2-$), 7.074–7.154 (d, $J_{cd} = 16$ Hz, 2H, $-CH=$), 7.852–7.933 (d, $J_{cd} = 16.2$ Hz, 2H, $-CH=$), 7.367–7.409 (d, $J_{ef} = 8.4$ Hz, 2H, Ar), 7.473–7.513 (d, $J_{ef} = 8.6$ Hz, 2H, Ar), 7.566 (4H, Ar), 7.975 (2H, Ar), 8.006–8.031 (2H, Pyr), 8.815–8.850 (d, $J_{ab} = 7$ Hz, 2H, Pyr), 9.019–9.052 (d, $J_{ab} = 6.6$ Hz, 4H, Pyr) |
| **A8** | $C_{42}H_{44}N_4Br_2$ | 764 | 208–215 | 1.874 (t, 4H, $-CH_2-$), 2.581 (s, 4H, $-CH_2-$), 2.682–2.741 (t, 4H, $-CH_2-$), 2.944 (s, 6H, $-CH_3$), 5.632 (s, 2H, $N^+CH_2-$), 5.768 (s, 2H, $N^+CH_2-$), 7.050–7.129 (d, $J_{cd} = 15.8$ Hz, 2H, $-CH=$), 7.812–7.892 (d, $J_{cd} = 16$ Hz, 2H, $-CH=$), 6.594–6.638 (d, $J_{ef} = 8.8$ Hz, 2H, Ar), 7.332–7.401 (3H, Ar), 7.553 (5H, Ar), 7.988–8.022 (d, $J_{ab} = 6.8$ Hz, 4H, Pyr), 8.790–8.824 (d, $J_{ab} = 6.8$ Hz, 2H, Pyr), 8.998–9.031 (d, $J_{ab} = 6.6$ Hz, 4H, Pyr) |
| **A9** | $C_{46}H_{48}N_4Br_2$ | 816 | 214–220 | 1.787–1.873 (m, 9H, $-CH_2-$), 2.581 (s, 6H, $-CH_2-$), 2.658–2.721 (t, 9H, $-CH_2-$), 5.607 (s, 2H, $N^+CH_2-$), 5.761 (s, 2H, $N^+CH_2-$), 6.984–7.063 (d, $J_{cd} = 15.8$ Hz, 2H, $-CH=$), 7.744–7.823 (d, $J_{cd} = 15.8$ Hz, 2H, $-CH=$), 7.136–7.202 (4H, Ar), 7.548 (4H, Ar), 7.933–8.002 (t, 4H, Pyr), 8.740–8.773 (d, $J_{ab} = 6.6$ Hz, 2H, Pyr), 8.993–9.026 (d, $J_{ab} = 6.6$ Hz, 2H, Pyr) |

maxima are red-shifted on increasing solvent polarity of about 20 nm (800 cm$^{-1}$) (see Table 2). A higher value of Stokes shift (>4000 cm$^{-1}$) is observed in acetonitrile and a lower valued (about 3000 cm$^{-1}$) in dichloromethane. This suggests that the Stokes shift increases on changing the solvent polarity. This behavior is a well-known manifestation of the charge transfer character of the solvent relaxed emissive state. The ICT state is derived following relaxation of the initially formed Franck–Condon excited state.

The fluorescence quantum yields of dimmers tested are very low and are dependent on the solvent polarity. In high polar solvent (acetonitrile) they have lower fluorescence quantum yields in comparison to medium polarity solvent such as dichloromethane.

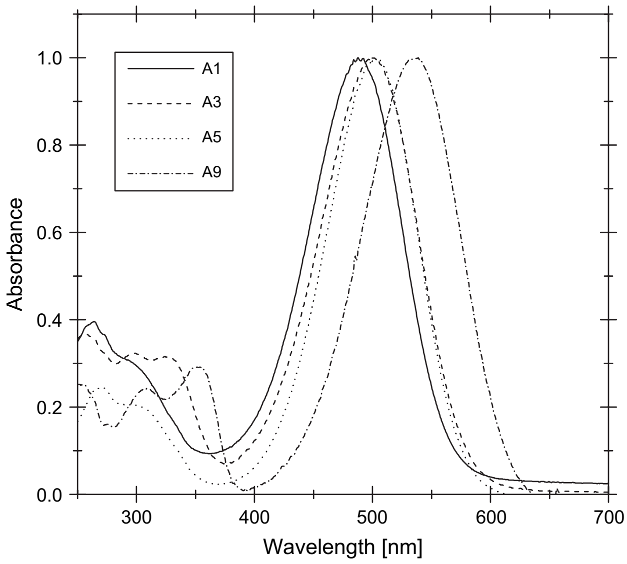

Fig. 1. Electronic absorption spectra of selected dimmers in acetonitrile at 293 K. The chromophores possess different donor groups (dye marked in the figure).

Table 2
Spectroscopic properties of the bichromophoric hemicyanine dyes tested in both dichloromethane and acetonitrile as the solvent

| Dye | $\lambda_{\max}^{\mathrm{Ab}}$ (nm), $\varepsilon$ ($\mathrm{M^{-1}\,cm^{-1}}$) | $^{\mathrm{Ab}}\nu/2$ ($\mathrm{cm^{-1}}$) | $\lambda_{\max}^{\mathrm{Fl}}$ (nm) | $^{\mathrm{Fl}}\nu/2$ ($\mathrm{cm^{-1}}$) | $\phi_{\mathrm{Fl}}$ | Stokes shift ($\mathrm{cm^{-1}}$) |
|---|---|---|---|---|---|---|
| Dichloromethane ($\epsilon = 8.93$, $n_{\mathrm{D}}^{20} = 1.42416$) | | | | | | |
| **A1** | 512 | 1532 | 617 | 754 | 0.076 | 3130 |
| **A2** | 524 | 1355 | 623 | 734 | 0.083 | 3030 |
| **A3** | 523 | 1511 | 620 | 791 | 0.025 | 2990 |
| **A5** | 528 | 1514 | 624 | 757 | 0.061 | 2790 |
| **A6** | 506 | 1890 | 628 | 796 | 0.063 | 3590 |
| **A7** | 537 | 1713 | 632 | 811 | 0.018 | 3300 |
| **A8** | 537 | 1450 | 633 | 796 | 0.026 | 3180 |
| **A9** | 565 | 1249 | 645 | 805 | 0.013 | 2420 |
| Acetonitrile ($\epsilon = 35.94$, $n_{\mathrm{D}}^{20} = 1.34411$) | | | | | | |
| **A1** | 487, 57 200 | 1628 | 632 | 733 | 0.0026 | 4690 |
| **A2** | 505, 83 500 | 1464 | 633 | 717 | 0.0038 | 4360 |
| **A3** | 499, 47 200 | 1621 | 634 | 679 | 0.0016 | 4270 |
| **A5** | 502, 92 900 | 1509 | 638 | 695 | 0.0025 | 4250 |
| **A6** | 481, 47 100 | 1905 | 640 | 731 | 0.0026 | 5190 |
| **A7** | 505, 25 900 | 1885 | 654 | 887 | 0.0012 | 4950 |
| **A8** | 511, 64 700 | 1554 | 650 | 802 | 0.0017 | 4280 |
| **A9** | 538, 72 400 | 1451 | 664 | 833 | 0.0013 | 3510 |

$^{\mathrm{Ab}}\nu/2$ ($\mathrm{cm^{-1}}$) and $^{\mathrm{Fl}}\nu/2$ ($\mathrm{cm^{-1}}$) are the half-widths of the absorption and fluorescence band, respectively.

It has been confirmed by several reports [17] that the formation of a nonradiative TICT state is the most efficient deactivation process of excited state of hemicyanine dyes. A polar solvent prefers the formation of the TICT state and this, in turn, increases the nonradiative transition of the excited state (lower values of the quantum yields of dimmers fluorescence in acetonitrile in comparison to dichloromethane, see Table 2).

The additional experimental evidence for the formation of nonradiative conformers in the excited state arises from the comparison of half-widths of both fluorescence and absorption bands (see Table 2). It is apparent from the inspection of the data collected in Table 2 that the emission spectra bands are somewhat narrower than the absorption ones. If the broadening of the spectra is understood as deriving from the population of the thermally available conformers, then according to Rettig and coworkers [18], the observed results can be taken as the evidence that some of these conformers are nonemissive (demonstrated by a reduction in fluorescence band width). The twisting of the olefinic double bands gives this type of a conformer. The deactivation of this state should occur mainly by radiationless processes because the energy gap between its excited state and the ground state is very small [18].

## 4. Summary

A series of hemicyanine dimmers have been synthesized and their steady-state absorption and fluorescence spectra

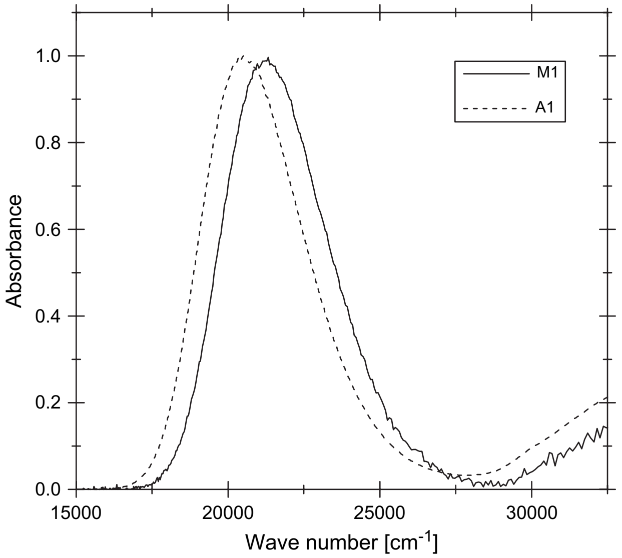

Fig. 2. Electronic absorption spectra of mono- (**M1**) and dichromophoric (**A1**) dyes (marked in the figure) in DMF at 293 K.

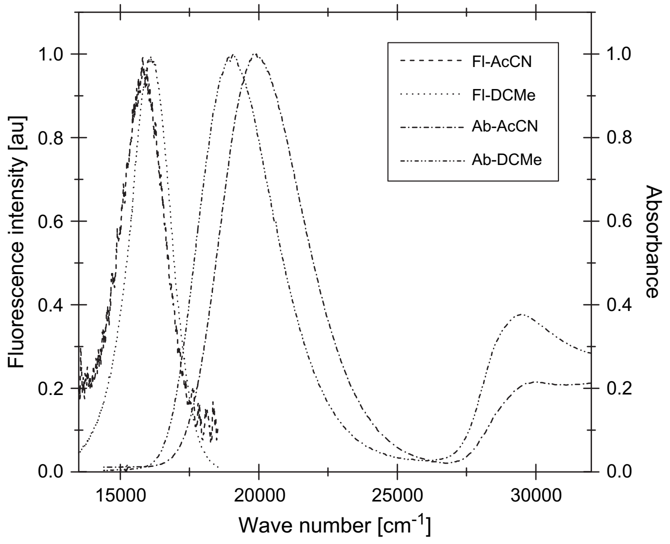

Fig. 3. Representative electronic absorption and fluorescence emission spectra of the **A2** dye. Spectra recorded in acetonitrile (AcCN) and dichloromethane (DCMe) at 293 K.

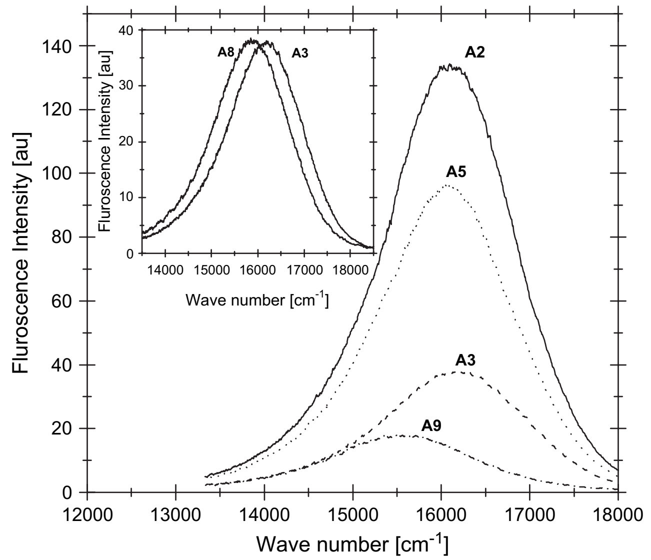

Fig. 4. Fluorescence emission spectra of the selected dyes. Spectra recorded in methylene dichloride at 293 K. Inset: Normalized fluorescence spectra of selected dyes illustrating the influence of the dye structure on the position of the emission maximum.

have been investigated. Negative solvatochromic behavior of absorption spectra is observed for all dyes. In high polar solvent (acetonitrile), all the dyes display low fluorescence quantum yields, whereas in a medium polarity solvent such as dichloromethane, the fluorescence quantum yield greatly increases (about one order of magnitude). The analysis of the fluorescence spectra in solvents of different polarity indicates the red-shift of the dimmers' emission maximum as the solvent polarity increases.

## Acknowledgment

This work was supported by the State Committee for Scientific Research (KBN) (Grants No 3T 09 B 101 28).

## References

[1] Ephardt H, Fromherz P. Fluorescence and photoisomerization of an amphiphilic aminostilbazolium dye as controlled by the sensitivity of radiationless deactivation to polarity and viscosity. J Phys Chem 1989;93:7717.

[2] Zhao CF, Gvishi R, Narang U, Ruland G, Prasad PN. Structures, spectra, and lasing properties of new (aminostyryl) pyridinium laser dyes. J Phys Chem 1996;100:4526–32.

[3] Gromov SP, Fedorova OA, Ushakov EN, Buevich AV, Baskin II , Pershina YV. J Am Chem Soc, Perkin Trans 2 1992:1323.

[4] He GS, Bhawalkar JD, Zhao CF, Prasad PN. Optical limiting effect in a two-photon absorption dye doped solid matrix. Appl Phys Lett 1995;67:2433–5.

[5] Mishra JK, Behera RK, Parida SK, Mishra BK. Ind J Chem 1992;31B:118.

[6] Zeena S, Thomas KG. Conformational switching and exciton interactions in hemicyanine-based bichromophores. J Am Chem Soc 2001; 123:7859.

[7] Huang Y, Cheng T, Li F, Huang C-H, Wang S, Huang W, et al. Photophysical studies on the mono- and dichromophoric hemicyanine dyes III. Ultrafast fluorescence up-conversion in methanol: twisting intramolecular charge transfer and "Two-State Three-Mode" model. J Phys Chem B 2002;106:10041–50.

[8] Gawinecki R, Andrzejak S, Puchała A. Efficiency of the Vilsmeier–Haack method in the synthesis of *p*-aminobenzaldehydes. Org Prep Proced Int 1998;30:455.

[9] Narang U, Zhao ChF, Bhawalkar JD, Bright FV, Prasad PN. Characterization of a new solvent-sensitive two-photon-induced fluorescent (aminostyryl) pyridinium salt dye. J Phys Chem 1996;100:4521–5.

[10] Ozçelik S. Steady state and picosecond time-resolved photophysics of a benzimidazolocarbocyanine dye. J Luminesc 2002;96:141–8.

[11] Mishra A, Haram NS. New push–pull type dendritic stilbazolium dyes: synthesis, photophysical and electrochemical investigation. Dyes Pigments 2004;63:191–202.

[12] Mishra JK, Behera RK, Behera GB. Ind J Chem 2000;39B:783.

[13] Mishra JK, Behera GB, Krishna MMG, Periasamy N. Time-resolved fluorescence studies of aminostyryl pyridinium dyes in organic solvents and surfactant solutions. J Luminesc 2001;92:175.

[14] Lang AD, Huang CH, Gan LB, Zhou DJ. Studies of the photocurrent generation performances from a series of amphiphilic bis-chromophore zinc complexes and correlation between photocurrent generation performance and molecular structure. Synth Met 1999;99:97–103.

[15] Huang Y, Cheng T, Li F, Luo C, Huang C-H, Cai Z, et al. Photophysical studies on the mono- and dichromophoric hemicyanine dyes II. Solvent effects and dynamic fluorescence spectra study in chloroform and in LB films. J Phys Chem B 2002;106:10031–40.

[16] Fromherz P. Monopole–dipole model for symmetrical solvatochromism of hemicyanine dyes. J Phys Chem 1995;99:7188–92.

[17] Fromherz P, Heilemann A. Twisted internal charge transfer in (aminophenyl) pyridinium. J Phys Chem 1992;96:6864–6.

[18] Szczepan M, Rettig W, Bricks YL, Słomiński YL, Tolmachev AI. Unsymmetric cyanines: chemical rigidization and photophysical properties. J Photochem Photobiol A 1999;124:75–84.